Intra-protein hydrogen bonding is dynamically stabilized by electronic polarization

Li L. Duan,[2] Ye Mei,[1] Qing G. Zhang,[2] and John Z. H. Zhang[1,3,a)]
[1]*Department of Physics, State Key Laboratory of Precision Spectroscopy, East China Normal University, Shanghai 200062, China*
[2]*College of Physics and Electronics, Shandong Normal University, Jinan 250014, China*
[3]*Department of Chemistry, New York University, New York, New York 10003, USA*

(Received 6 January 2009; accepted 5 February 2009; published online 19 March 2009)

Molecular dynamics (MD) simulation has been carried out to study dynamical stability of intra-protein hydrogen bonds based on two set of atomic charges, the standard AMBER charge and the polarized protein-specific charge (PPC). The latter is derived from quantum mechanical calculation for protein in solution using a recently developed molecular fractionation with conjugate caps-Poisson-Boltzmann (MFCC-PB) approach and therefore includes electronic polarization effect of the protein at native structure. MD simulations are performed for a number of benchmark proteins containing helix and/or beta sheet secondary structures. The computational result shows that occupancy percentage of hydrogen bonds averaged over simulation time, as well as the number of hydrogen bonds as a function of simulation time, is consistently higher under PPC than AMBER charge. In particular, some intra-protein hydrogen bonds are found broken during MD simulation using AMBER charge but they are stable using PPC. The breaking of some intra-protein hydrogen bonds in AMBER simulation is responsible for deformation or denaturing of some local structures of proteins during MD simulation. The current study provides strong evidence that hydrogen bonding is dynamically more stable using PPC than AMBER charge, highlighting the stabilizing effect of electronic polarization on protein structure. © *2009 American Institute of Physics*. [DOI: 10.1063/1.3089723]

I. INTRODUCTION

Molecular FF (FF) has played an indispensable role in theoretical studies of biology and provided important information about structure and dynamics of proteins. Molecular dynamics (MD) simulation based on these FF such as CHARMM, AMBER, etc., has been widely employed to extract information on time evolution of protein conformations and has contributed significantly to our understanding of biological processes at detailed molecular levels.[1–6] MD simulation provides direct observation of protein's dynamic behavior and uncovers important roles that dynamics played in processes such as protein folding, protein-ligand interaction, etc. In addition, MD simulation provides an efficient means for sampling structures needed for computing thermodynamic properties of proteins such as ionization constant for ionizable amino acids in proteins, reaction energy barrier of chemical process catalyzed by enzyme, and free energy landscape of protein folding.

However, the accuracy of dynamic properties derived from MD simulation depends on the accuracy of the FF employed. For example, protein's stable structure is determined by detailed balance of inter-residue interaction and protein-solvent interaction. These noncovalent interactions are relatively weak, and earlier study in mutation and crystallography experiments suggests that perturbation of small part of these interactions may cause large conformational change in protein's structures. This implies that small inaccuracy in the FF may introduce significant conformation errors during MD simulations. A well-known deficiency of the widely used FF is the lack of electronic polarization of proteins. Specifically, the currently employed atomic charges in the standard FF are based on fitting of electrostatic potential (ESP) of individual amino acids, without the polarization effect of the protein. Since electrostatic interaction plays a major role in protein interaction, the lack of protein polarization could be reflected in deficiencies in some structural details and dynamical properties extracted from MD simulations.

In this work, we explore polarized protein-specific charge (PPC) based on quantum chemistry calculation of the entire protein in solution and such calculation is made possible by using the molecular fractionation with conjugate caps[7–13] (MFCC) approach incorporating the Poisson-Boltzmann (PB) equation to treat protein in solvent.[14,15] Thus PPCs are protein specific which distinguishes them from amino acid-specific charges typically used in existing FFs such as AMBER. These features of PPC imply that they should provide more accurate electrostatic interactions for proteins near the native structures. This is extremely important since electrostatic interaction plays a significant role in protein structure and function.[16–20] Processes such as protein folding, protein-ligand binding, protein-protein interaction, electron transfer, proton binding release, enzyme reaction, etc., are largely driven by electrostatic interactions. Since PPC is obtained by charge fitting to ESP from quantum mechanical calculation of the entire protein at native structure,

a)Electronic mail: john.zhang@nyu.edu.

it contains the proper polarization effect and should provide more reliable description of protein dynamics at and near the native structure. Because PPC also features fixed atomic charges, its application is most straightforward and is entirely compatible with the existing FF for MD simulations and other applications.[21] Recently study shows that PPC gives more stable protein dynamics.[21,22]

The present work is focused on studying dynamical stability of intra-protein hydrogen bonds (H-bonds) and secondary structures for a number of benchmark proteins including thioredoxin, staphylococcal nuclease, ubiquitin, lysozyme, ribonuclease T1, and crambin using both PPC and AMBER charge. Thioredoxin (TRX) is a well-known enzyme that is present in all living organisms[23] and contain a disulfide bridge involved in several metabolic function inside and outside the cells.[24] Thioredoxin plays an essential role in cell function by limiting oxidative stress directly via antioxidant effects and indirectly by protein-protein interactions with key signaling molecular.[25] Staphylococcal nuclease consists of an "OB-fold" flanked by two α-helices, the OB-fold consists of a α-helix and of a five-stranded Greek-key β-barrel[26] and has been used in several significant studies as a model such as structure-function relationships, protein folding.[27] Ubiquitin is a small protein which is composed of 76 amino acids and its core is composed of an α-helix and a β-sheet; ubiquitin is involved in many cell process and the most prominent function is to mark other proteins for destruction such as proteolysis. Lysozyme is a single chain of 129 residues which folds into a compact globular structure and consists of five to seven α-helix and a three-stranded antiparallel β-sheet. It is found mainly in egg whites, tears, and various other secretions of eukaryotic cells.[28] Ribonuclease T1 is a small single-domain protein containing 104 amino acids and the native structure consists of a four- and five-turn α-helix packed against a central five-strand antiparallel β-sheet.[29] Crambin contains three disulfide bonds, an α-helix, a β-sheet, and a reverse turn. It is isolated from the seeds of the plant Crambe abyssinica[30] that has no known biological function. All six proteins are excellent test systems because they have been extensively studied both experimentally and theoretically.

II. THEORETICAL METHODS

A. Generation of PPC

Since the procedure to compute PPC for a given protein structure is already reported elsewhere,[21] we give only a brief review of the method here. The basic procedures in fitting atomic charges of protein in our approach can be described as follows: First, gas phase quantum chemistry calculation of protein is performed with the MFCC approach to obtain initial electron density of the protein through fragment calculation for the given structure as described earlier.[7,10,11] The calculated electron density is used to fit atomic charges using the restrained electrostatic potential (RESP) procedure. Charge fitting philosophy used here was the same as that used in AMBER FF and this guarantees that PPC charge is consistent with other parameters of AMBER FF. Solution of PB equation is then carried out to obtain reaction field and from which to generate discrete surface charges on the cavity surface. The quantum chemistry calculation of protein fragment is performed again but now with the protein embedded in an external ESP produced by induced solvent surface charges and other fragments of the protein.[11,21] The newly calculated protein atomic charges are used again to calculated new solvent induced charges and such processes are repeated until convergence is reached. The quantum chemistry calculation is performed at the level of B3LYP/6-31G*.

B. MD simulation

The initial structures of thioredoxin (PDB entry 1XOA), staphylococcal nuclease (PDB entry 1SNO), ubiquitin (PDB entry 1D3Z), lysozyme (PDB entry 1E8L), ribonuclease T1 (PDB entry 1YGW), and crambin (PDB entry 2EYA) which include helix and sheet structures are taken as the starting structure. Then MD simulations are performed using the AMBER 9 suite of programs with 2003 FF and PPC, respectively. When performing simulation with PPC, the AMBER charges are simply replaced by the PPC while the rest of the FF parameters are retained. In MD simulation, the protein is placed in a truncated octahedral periodic box of TIP3P water molecular. The distance from the surfaces of the box to the closest atoms of the solutes is set to 12 Å. Counterions are added to neutralize the system. The complete system is energy minimized by the steepest descent method followed by conjugate gradient minimization. The system is then heated from 0 to 300 K over 300 ps with harmonic constraints on all solute atoms and the Langevin dynamics with a collision frequency of 1.0 ps^{-1} are used to regulate the temperature. Finally MD simulation is performed in *NPT* ensemble to further relax the system without any restraints on solute atoms. In MD simulations, SHAKE[31] algorithm is used to constrain all the bonds involving hydrogen atoms, and the time step is 2 fs.

III. RESULTS AND DISCUSSIONS

For proteins in their native structures, H-bonds are the main driving force to stabilize, e.g., helix, β-sheet, and other secondary structures and therefore play a vital role in intramolecular and intermolecular interactions in biological systems. With respect to their precise roles in protein folding and protein stability as well as in protein recognition,[32–34] the properties of hydrogen bonds have been studied for decades and continue to be a focus of many theoretical and experimental interests. Therefore, appropriate representation of H-bonds is essential to our ability in protein structure prediction, protein-protein docking, protein design, and protein-ligand interactions.[35] H-bonds are dominated by electrostatic interaction. Because PPC properly describes polarized electrostatic state of the protein in a given (native) structure, we expect that it will provide more accurate description on hydrogen bonding at or near the native structure. Therefore some difference in structural details of the protein should be observed in MD simulation between using PPC and AMBER03 charge. For that purpose, we carried out MD calculations for six proteins employing separately PPC and AMBER03 charge to study dynamical structural differences.

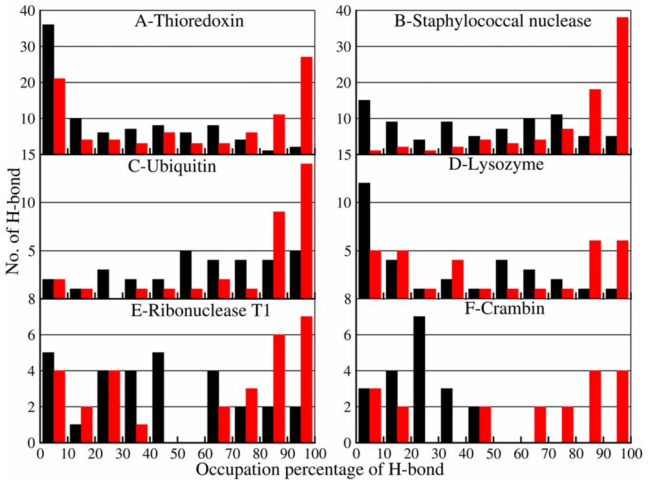

FIG. 1. (Color online) Comparison of occupation percentage of H-bonds from MD simulation using AMBER03 (black) and PPC (red), respectively, for six proteins: thioredoxin (a), staphylococcal nuclease (b), ubiquitin (c), lysozyme (d), ribonuclease T1 (e), and crambin (f). The occupation percentage is averaged over time after the equilibrium is reached in MD simulation.

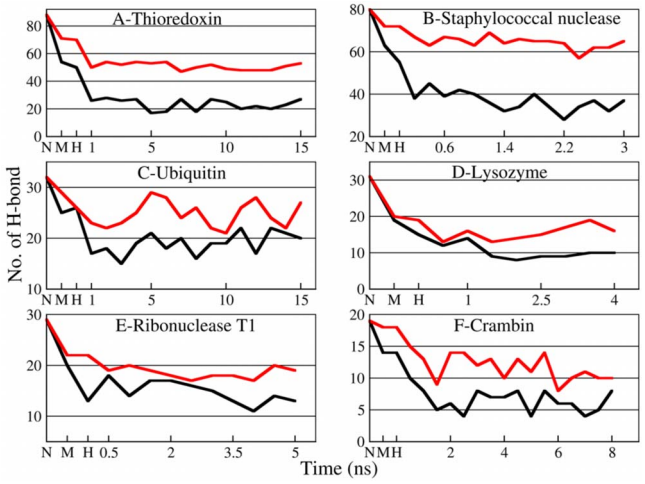

FIG. 2. (Color online) Comparison of the number of H-bonds as a function of MD simulation time using AMBER03 (black) and PPC (red), respectively, for six proteins: thioredoxin (a), staphylococcal nuclease (b), ubiquitin (c), lysozyme (d), ribonuclease T1 (e), and crambin (f). H-bond is defined such that the distance between N and O is less than 3.0 Å and the angle N–H–O is larger than 120.0°. "N" denotes the number of H-bonds in NMR structure. "M" denotes the number of H-bonds after minimization. "H" denotes the number of H-bonds after heating.

The initial structures of thioredoxin, staphylococcal nuclease, ubiquitin, lysozyme, ribonuclease T1, and crambin have 88, 80, 32, 31, 29, and 19 H-bonds, respectively. The number of H-bonds is defined as the number of all H-bonds formed from standard amino acids. A H-bond is counted if the distance between two heavy atoms (N and O in this case) is less than 3.0 Å and the angle N–H–O is larger than 120.0° in standard definition. We first compare the stability of H-bonds during MD simulation after initial period of stability is reached. Specifically, we performed statistical analysis of the number of H-bonds to examine the percentage occupancy of them from MD simulation. For example, if a particular H-bond remains intact during 95% of the simulation time, its occupation percentage is 95%, and the numbers of H-bonds can be grouped within a certain occupation percentage range such as from 90% to100%. We can therefore plot a histogram to show fractions of these H-bonds versus their occupancy. Figure 1 shows the comparison of H-bond distributions obtained from MD simulations using PPC and AMBER03 charge, respectively, for these six proteins. A critical difference is observed in Fig. 1. Starting from the same NMR structure, the distribution of H-bonds based on simulation using PPC is composed preferentially of high occupancy H-bonds. In contrast, the distribution based on simulation using AMBER03 charge is dominated by low occupancy H-bonds. In all six proteins, the ratios of proportions of H-bonds in high occupancy (80%–100%) to the total H-bonds between AMBER03 charge and PPC are about 0.03/0.43, 0.13/0.70, 0.28/0.72, 0.06/0.39, 0.14/0.45, and 0/0.42, respectively. High occupancy H-bond means more stable H-bonds in protein dynamics. Our study shows that using PPC in MD simulation, a majority of H-bonds appearing in the NMR structure remains intact in MD simulation. The results are not too surprising in view of the difference between PPC and AMBER03 charge. Since the formation of internal H-bonds in protein polarizes the donors and acceptors, this polarization effect is better represented by PPC than by AMEBR03 charge. As a result, the H-bonds in proteins are generally more stable during MD calculations. Overall, the PPCs are close to the result of experiment in the statistical analysis of the number of H-bonds. This is expected to be a general feature of the PPC since they correctly represent the polarized electrostatic effect of the protein.

We further study the time dependence of the number of H-bonds as a function of MD simulation time for six proteins. The result is shown in Fig. 2 using AMEBR03 charge and PPC, respectively. As previously, the H-bond is defined for distance between N and O being less than 3.0 Å and the angle N–H–O being larger than 120.0°. Although after initial minimization and heating, the number of H-bond is initially reduced over simulation time, more H-bonds are preserved in PPC than in AMBER03 simulation. Since the definition for H-bond is not as rigid, we broaden the definition for H-bond by increasing the distance between N and O to 3.5 Å. After relaxation of distance for H-bond definition, the number of

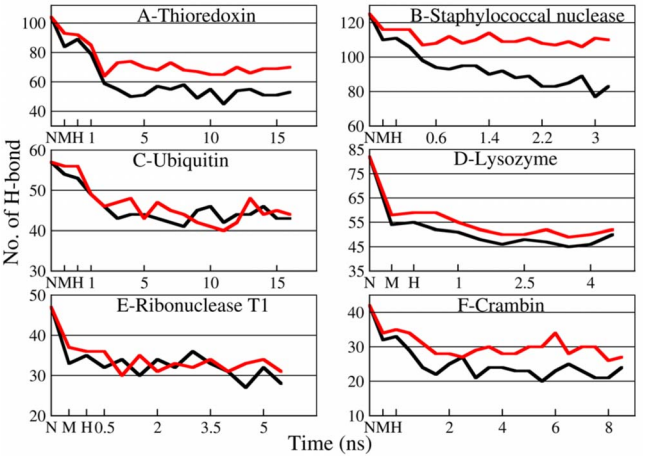

FIG. 3. (Color online) Same as Fig. 2 except for the definition of H-bond in which the maximum distance between N and O is increased to 3.5 Å.

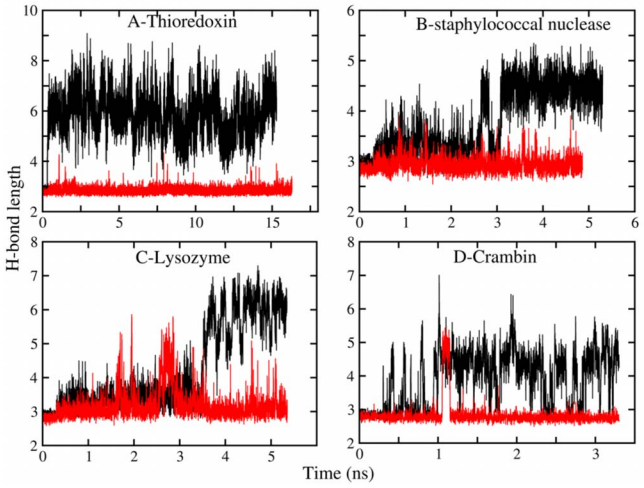

FIG. 4. (Color online) Evolution of backbone H-bond length using, respectively, AMBER03 charge (black) and PPC (red) in MD simulation. (a) H-bond between Asp13 and Lys18 in thioredoxin. (b) H-bond between Ile13 and Thr17 in staphylococcal nuclease. (c) H-bond between Cyx115 and Thr118 in lysozyme. (d) H-bond between Thr1 and Ile35 in crambin.

H-bonds in respective NMR structures is now increased to 104, 125, 57, 82, 47, and 42 H-bonds for six proteins, respectively. Figure 3 plots the time dependence of the number of H-bonds using this relaxed definition. Obviously, the overall number of H-bonds in these systems is increased with this relaxed condition as shown in Fig. 3. With the exception of ubiquitin and ribonuclease T1, the relative difference in the number of H-bonds between simulations using PPC and AMBER03 charge remains similar. The results in Fig. 3 are consistent with those of Fig. 2 indicating that small change in H-bond definition does not make material difference.

We also investigate the time evolution of individual backbone H-bonds during MD simulation using AMBER03 charge and PPC as shown in Fig. 4. The specific backbone H-bonds (between pairs of Asp13 and Lys18 in thioredoxin, Ile13-Thr17 in staphylococcal nuclease, Cyx115-Thr118 in lysozyme, and Thr1-Ile35 in crambin) are well preserved during MD simulation using PPC. As shown in Fig. 4, the length of the corresponding H-bond in each of these four proteins remains close to the value in NMR structure over the entire simulation time, indicating that the H-bond remains stable. However, the very same H-bonds either break or undergoing large fluctuation when AMBER charge is used in simulation. For example, the backbone H-bond between Asp13 and Lys18 in thioredoxin breaks rather quickly after simulation starts as shown in Fig. 4(a). In comparison, the backbone H-bond between Ile13 and Thr17 in staphylococcal nuclease and that between Cyx115 and Thr118 in lysozyme breaks after about 3 ns simulation time [see Fig. 4(b) and 4(c)]. On the other hand, the H-bond length between Thr1 and Ile35 in crambin undergoes large fluctuation after about 0.4 ns simulation [Fig. 4(d)].

Of course, examining the distribution of occupancy of individual H-bonds does not necessarily provide a complete view of the influence of electrostatic polarization on important motifs or substructures which are more important in determining the overall structure and function of protein. Since these backbone H-bonds lie inside either helix or sheet or other local secondary structures in these proteins, it is useful

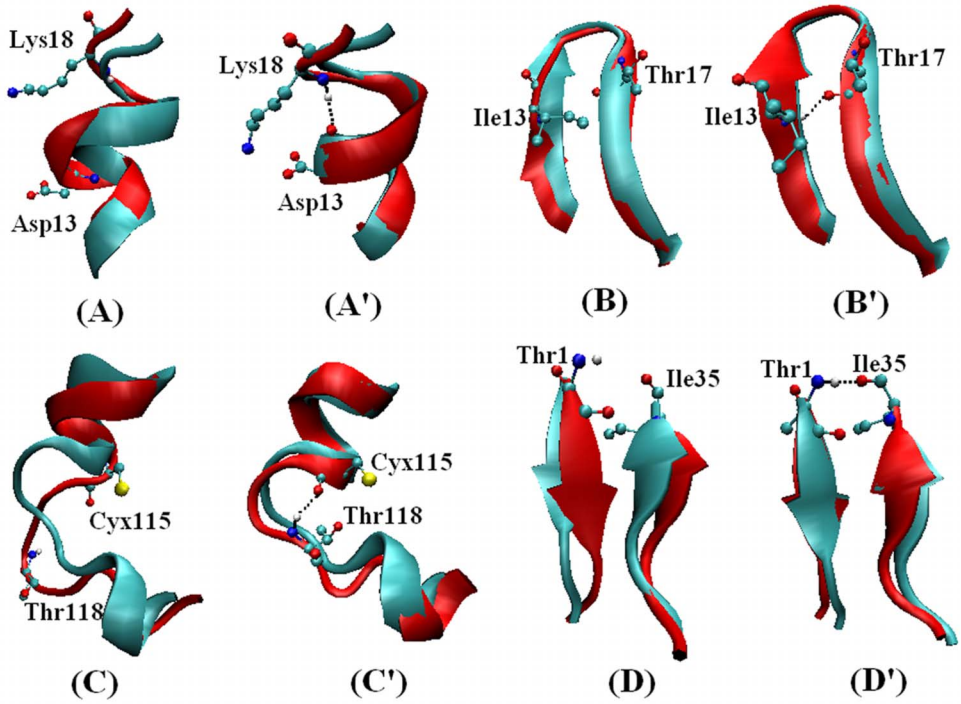

FIG. 5. (Color online) Comparison of the corresponding secondary structure containing the H-bonds in Fig. 4 between AMBER03 simulation (red) and NMR (cyan) and between PPC simulation (red) and NMR (cyan). Secondary structure is averaged over the last 200 ps in MD simulation. (a) Corresponding secondary structure of thioredoxin between AMBER03 charge simulation and NMR. (a') Same as in (a) but for PPC. (b) Same as in (a) but for staphylococcal nuclease. (b') Same as in (b) but for PPC. (c) Same as in (a) but for lysozyme. (c') Same as in (c) but for PPC. (d) Same as in (a) but for crambin. (d') Same as in (d) but for PPC.

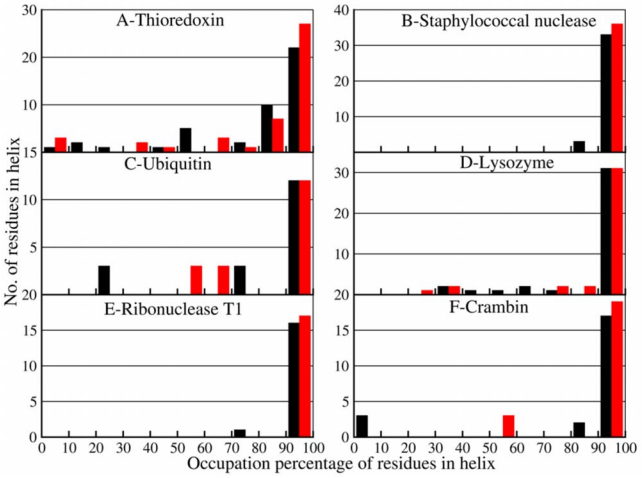

FIG. 6. (Color online) Comparison of occupation percentage of residues in helix from MD simulation using AMBER03 (black) and PPC (red), respectively, for six proteins: thioredoxin (a), staphylococcal nuclease (b), ubiquitin (c), lysozyme (d), ribonuclease T1 (e), and crambin (f). The occupation percentage is averaged over time after the equilibrium is reached in MD simulation.

to examine whether the breaking of these H-bonds results in any change in these secondary structures. For this purpose, we plot in Fig. 5 the comparison between two sets of final structures of four proteins resulting from MD simulation using AMBER and PPC, respectively. These structures are obtained by averaging the corresponding protein structures over the final 0.2 ns time frame. The specific H-bond that is broken in AMBER charge but intact in PPC is explicitly shown in Fig. 5 for clarity. Observable changes in detailed structures are seen in Fig. 5. For example, the breaking of the backbone H-bond between Asp13 and Lys18 in thioredoxin in MD simulation using AMBER charge resulted in some deformation of the corresponding helix structure as shown in Figs. 5(a) and 5a′. Similarly, the breaking of H-bond between Cyx115 and Thr118 resulted in deformation of the hinge region in lysozyme during MD simulation using AMBER charge as shown clearly in Fig. 5. Some changes in sheet structures are also seen in Fig. 5 for staphylococcal nuclease and crambin due to breaking of backbone H-bond when AMBER charge is used in MD simulation as shown in Fig. 5. However, the changes in sheet structures seem to be less prominent as in helix structures. Clearly MD simulation using PPC better preserves secondary structures and thus should give more stable dynamical structure of the protein.

We also performed statistical analysis to examine the occupation percentage of secondary structures from MD calculations. The defined secondary structure of proteins (DSSP) (Ref. 36) method is used to identify secondary structure elements in protein structures. The distributions of residues in helix and sheet obtained from MD simulation between AMBER charge and PPC are shown in Figs. 6 and 7, respectively. The results are obviously consistent with the above analysis, showing more stable secondary structures when PPC is used for simulation. Figures 6 and 7 show that the polarization effect on sheet structure is relatively weaker than on helix, consistent with those observed in Fig. 5.

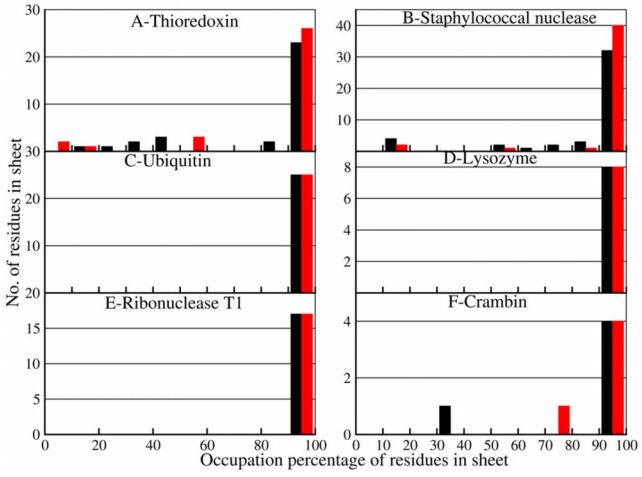

FIG. 7. (Color online) Comparison of occupation percentage of residues in β-sheet from MD simulation using AMBER03 (black) and PPC (red), respectively, for six proteins: thioredoxin (a), staphylococcal nuclease (b), ubiquitin (c), lysozyme (d), ribonuclease T1 (e), and crambin (f). The occupation percentage is averaged over time after the equilibrium is reached in MD simulation.

IV. CONCLUSIONS

In this paper, we employed the recently developed MFCC approach coupled with implicit treatment of solvent to generate PPCs for MD simulation of six benchmark small proteins to investigate the polarization effect on hydrogen bonding in secondary structures for comparison with results obtained from using standard AMBER charge. The results clearly shows that H-bonds and secondary structures are more stable and better preserved in MD simulation employing PPC than AMBER charge. In particular, our result shows that MD simulation using standard AMBER charge can break some backbone hydrogen bonds in secondary structures and result in structural deformation. The current result is a further demonstration that PPC provides superior alternative to standard charge for MD simulation of protein at and near the native structure and could avoid incorrect deformation of protein structure, which has been recently observed in dynamical motion of PPAR-γ.

It should be mentioned that somewhat related idea or methods have been reported that share some of the flavors of the current approach in which electron polarization and structure-based quantum calculations are treated in some effective way for MD simulations.[37–39] The development of new generation quantum methods for protein structure calculation should enable us to provide new insight as well as more accurate description of protein structure and dynamics in computational biology.

ACKNOWLEDGMENTS

This Project is supported by the National Basic Research Program of China (Grant No. 2004CB719901), the National Natural Science Foundation of China (Grants No. 10874104 and 20773060), the Natural Science Foundation of Shandong Province (Grant No. Z2007A05), and the Scientific Research Award for the Excellent Middle-Aged and Young Scientists of Shandong Province (Grant No. 2008BS01013). J.Z.H.Z. is

partially supported by the Petroleum Research Fund (Grant No. 44056-AC6) administered by the American Chemical Society.

[1] A. T. Hagler, E. Huler, and S. Lifson, J. Am. Chem. Soc. **96**, 5319 (1974).
[2] B. R. Brooks, R. E. Bruccoleri, B. D. Olafson, D. J. States, S. Swaminathan, and M. Karplus, J. Comput. Chem. **4**, 187 (1983).
[3] G. Nemethy, M. S. Pottle, and H. A. Scheraga, J. Phys. Chem. **87**, 1883 (1983).
[4] H. J. C. Berendsen, J. P. M. Postma, W. F. v. Gunsteren, A. diNola, and J. R. Haak, J. Chem. Phys. **81**, 3684 (1984).
[5] D. A. Pearlman, D. A. Case, J. W. Caldwell, W. S. Ross, T. E. Cheatham III, S. DelBolt, G. Seibel, and P. Kollman, Comput. Phys. Commun. **91**, 1 (1995).
[6] S. A. Adcock and J. A. McCammon, Chem. Rev. (Washington, D.C.) **106**, 1589 (2006).
[7] D. W. Zhang and J. Z. H. Zhang, J. Chem. Phys. **119**, 3599 (2003).
[8] X. He, Y. Mei, Y. Xiang, D. W. Zhang, and J. Z. H. Zhang, Proteins: Struct., Funct., Bioinf. **61**, 423 (2005).
[9] Y. Mei, X. He, Y. Xiang, D. W. Zhang, and J. Z. H. Zhang, Proteins: Struct., Funct., Bioinf. **59**, 489 (2005).
[10] Y. Mei, D. W. Zhang, and J. Z. H. Zhang, J. Phys. Chem. A **109**, 2 (2005).
[11] Y. Mei, C. G. Ji, and J. Z. H. Zhang, J. Chem. Phys. **125**, 094906 (2006).
[12] Y. Mei, E. L. Wu, K. L. Han, and J. Z. H. Zhang, Int. J. Quantum Chem. **106**, 1267 (2006).
[13] L. L. Duan, Y. Tong, Y. Mei, Q. G. Zhang, and J. Z. H. Zhang, J. Chem. Phys. **127**, 145101 (2007).
[14] B. Honig, K. A. Sharp, and A.-S. Yang, J. Phys. Chem. **97**, 1101 (1993).
[15] D. J. Tannor, B. Marten, R. Murphy, R. A. Friesner, D. Stikoff, A. Nicholls, M. Ringalda, W. A. Goddard III, and B. Honig, J. Am. Chem. Soc. **116** 11875 (1994).
[16] M. Perutz, Science **201**, 1187 (1978).
[17] A. Warshel and S. Russell, Q. Rev. Biophys. **17**, 283 (1984).
[18] J. B. Matthew, Annu. Rev. Biophys. Biophys. Chem. **14**, 387 (1985).
[19] M. E. Davis and J. A. McCammon, Chem. Rev. (Washington, D.C.) **90**, 509 (1990).
[20] B. Honig and A. Nicholls, Science **268**, 1144 (1995).
[21] C. G. Ji, Y. Mei, and J. Z. H. Zhang, Biophys. J. **95**, 1080 (2008).
[22] C. G. Ji and J. Z. H. Zhang, J. Am. Chem. Soc. **130**, 17129 (2008).
[23] H. Ming, Y. Kato, K. Miyazono, K. Ito, M. Kamo, K. Nagata, and M. Tanokura, Proteins: Struct., Funct., Bioinf. **69**, 204 (2007).
[24] J.-M. Lancelin, L. Guilhaudis, I. Krimm, M. J. Blackledge, D. Marion, and J.-P. Jacquot, Proteins **41**, 334 (2000).
[25] H. Yamawaki and B. C. Berk, Curr. Opin. Nephrol. Hypertens. **12**, 149 (2005).
[26] A. T. Alexandrescu, W. Jahnke, R. Wiltscheck, and M. J. J. Blommers, J. Mol. Biol. **260**, 570 (1996).
[27] J. L. Markley, A. P. Hinck, S. N. Loh, K. Prehoda, D. Truckses, W. F. Walkenhorst, and J. Wang, Pure Appl. Chem. **66**, 65 (1994).
[28] J. Pooart, T. Torikata, and T. Araki, Biosci., Biotechnol., Biochem. **68**, 159 (2004).
[29] J. B. Garrett, L. S. Mullins, and F. M. Raushel, Protein Sci. **5**, 204 (1996).
[30] D. Bang, N. Chopra, and S. B. H. Kent, J. Am. Chem. Soc. **126**, 1377 (2004).
[31] J. P. Ryckaert, G. Ciccotti, and H. J. C. Berendsen, J. Comput. Phys. **23**, 327 (1977).
[32] K. A. Dill, Biochemistry **29**, 7133 (1990).
[33] B. Honig and A. S. Yang, Adv. Protein Chem. **46**, 27 (1995).
[34] J. K. Myers and C. N. Pace, Biophys. J. **71**, 2033 (1996).
[35] B. D. Hames, N. M. Hooper, and J. D. Houghton, *Instant Notes in Biochemistry* (BIOS Scientific, Oxford, 1997).
[36] W. Kabsch and C. Sander, Biopolymers **22**, 2577 (1983).
[37] J. L. Gao, F. J. Luque, and M. Orozco, J. Chem. Phys. **98**, 2975 (1993).
[38] W. S. Xie and J. L. Gao, J. Chem. Theory Comput. **3**, 1890 (2007).
[39] W. S. Xie, L. C. Song, D. G. Truhlar, and J. L. Gao, J. Phys. Chem. B **112**, 14124 (2008).